Available online at www.sciencedirect.com
ScienceDirect
Materials Science and Engineering C 27 (2007) 251–256
MATERIALS SCIENCE & ENGINEERING C
www.elsevier.com/locate/msec

# Silicon-substituted hydroxyapatite: The next generation of bioactive coatings

E.S. Thian *, J. Huang, S.M. Best, Z.H. Barber, W. Bonfield

*Department of Materials Science and Metallurgy, University of Cambridge, Pembroke Street, Cambridge, CB2 3QZ, UK*

Received 8 July 2005; accepted 3 March 2006
Available online 9 June 2006

## Abstract

Silicon-substituted hydroxyapatite (Si–HA) coatings with three different Si compositions (0.8, 2.2 and 4.9 wt.%) were produced as thin films on titanium substrates by magnetron co-sputtering. Following heat-treatment, a crystalline, single-phase apatite structure was obtained for all coatings, as evidenced by the presence of characteristic peaks for HA in X-ray diffraction traces, and infrared absorption P–O and O–H bands. A human osteoblast-like (HOB) cell model was employed to assess the biocompatibility of these Si–HA coatings. Unsubstituted HA thin coatings were used as a control. The results demonstrated that Si–HA elicited a significantly more rapid growth response by the HOBs as compared to HA, although cells spread well on both coatings, with the formation of extracellular matrix. The cytoskeletons on Si–HA showed clear and distinct actin filaments that were parallel to the long axis of the cells. In contrast, a more diffuse actin cytoskeleton organisation was observed on HA. Biomineralisation was seen on both coatings after 42 days of culturing, with a higher level observed on the Si–HA samples. In conclusion, Si–HA offers great potential as a coating material for future medical applications in hard and soft tissue replacements.


*Keywords:* Coatings; Silicon; Hydroxyapatite; Osteoblasts; Actin; Biomineralisation

## 1. Introduction

Calcium phosphate (CaP) materials have been widely used for bone replacement in dental, facial and orthopaedic applications. A number of features make CaP an ideal biomaterial including the ability to (1) form strong interfacial bonds with bone tissue without fibrous encapsulation; (2) facilitate the growth of bone tissue so as to achieve early mechanical bone fixation; and (3) act as a scaffold on which bone-forming cells (osteoblasts) can attach, grow, divide and form new bone [1]. Hydroxyapatite [HA, $Ca_{10}(PO_4)_6(OH)_2$] is the most commonly used CaP-based biomaterial due to its similarity in composition and structure to bone mineral [2]. The use of HA as coatings on femoral stems of total hip joint implants in humans was first reported by Furlong and Osborn [3]. Since then, it has been used extensively in both dental and orthopaedic implants.

Developments in bioactive coatings have led to an improvement in the overall performance of coated biomedical implants. Delecrin et al. [4] showed that a biphasic CaP coating, a mixture containing 60 wt.% HA and 40 wt.% beta-tricalcium phosphate (β-TCP), led to faster bone formation in rabbits than HA coatings in-vivo. Since TCP is a highly bioresorbable material, there has been some discussion in the literature concerning the use of TCP. However, Klein et al. [5] demonstrated that TCP was not an ideal coating material due to the fact that resorption occurred before bone ingrowth was sufficient to ensure proper fixation. Bioglass® coatings, developed by Lacefield and Hench [6], have demonstrated the capability of bonding directly to bone, so as to be used in load bearing applications. Recently, two independent in-vitro studies indicated that bioactive glass coatings have positive stimulating effects towards osteoblast proliferation and differentiation [7,8]. However, a potential disadvantage is that the presence of high levels of released silica ions from the coating at a local level could be toxic to the surrounding tissues [9].

Another approach is to incorporate biological entities such as transforming growth factors (capable of stimulating cell proliferation and differentiation) or bone morphogenetic proteins (capable of inducing rapid bone formation) onto the HA coating

* Corresponding author. Tel.: +44 1223 334560; fax: +44 1223 334567.
*E-mail address:* est23@cam.ac.uk (E.S. Thian).

0928-4931/$ - see front matter © 2006 Elsevier B.V. All rights reserved.
doi:10.1016/j.msec.2006.05.016

Table 1
Fabrication of Si–HA thin coatings

| $T_e$ (°C) | $T$ (h) | dc (W) | rf (W) | $t$ (μm) | Si (wt.%) |
|---|---|---|---|---|---|
| 600 | 3 | 3 | 60 | 0.7 | 0.8 |
| | | 9 | | | 2.2 |
| | | 15 | | | 4.9 |

$T_e$: heat-treatment temperature.
$T$: heat-treatment duration.
dc: direct current power at Si target.
rf: radio frequency power at HA target.
$t$: coating thickness.

surfaces, to accelerate the biological fixation [10–12]. However, storage and sterilisation processes have been reported to reduce the beneficial effects of these bioactive agents [13].

We have recently proposed and developed a novel chemically modified apatite: silicon-substituted HA (Si–HA) as a bioactive coating, to be used in bone-related applications [14,15]. The speculation that Si plays an important role in connective tissue metabolism is supported by Carlisle who demonstrated that chicks fed with unsupplemented Si diets showed reduced growth, diminished feather development, and significantly retarded skeletal development [16–18].

There are several available techniques to apply Si–HA coatings onto implant surfaces. In our study, magnetron co-sputtering coupled with appropriate heat-treatment, was used. The application of this technique is novel, and allows the establishment of uniform, dense and well-adhered thin coatings, with the possibility of the addition of controlled levels of Si. The ability to achieve thin coatings (~ 1 μm) may reduce the risk of coating delamination or fracture when the coated prostheses are press fitted into the implantation site. This effect may reduce third body wear from occurring since the presence of embedded foreign particles at the interface will lead to implant loosening and failure with time [19]. The aim of this paper is to provide a brief overview of Si–HA coating in terms of its physical, chemical and biological characterisation.

## 2. Materials and methods

### 2.1. Materials

Pure titanium (Ti) substrates measuring 10 × 5 × 0.5 mm, were used. They were ground using silicon carbide paper of grade 1200 and ultrasonically cleaned with acetone before rinsing with deionised water. Pure silicon (Si) and phase-pure sintered hydroxyapatite (HA) measuring 55 × 35 × 2 mm, were used as the sputtering targets.

### 2.2. Magnetron co-sputtering

Deposition of silicon-substituted hydroxyapatite (Si–HA) thin coatings was conducted at room temperature. Si and HA targets were held onto two water-cooled magnetrons, and Ti substrates were placed on a substrate holder facing the targets. The target–target and target–substrate distances were fixed at 105 and 45 mm, respectively. For each deposition run, a constant flow of high purity argon (Ar) gas was supplied to the chamber, bringing the working pressure to 0.6 Pa. A sputtering time of 4 h was used. A radio frequency (rf: 13.56 MHz) power of 60 W was supplied to the HA target, and three varying direct current (dc) powers of 3, 9 and 15 W were supplied to the Si target in order to achieve coatings with three different Si contents. These as-sputtered coatings were then heat-treated at 600 °C for 3 h under a water vapour-Ar atmosphere.

### 2.3. Physicochemcial characterisation of heat-treated Si–HA

The thickness of the coating was determined by masking a portion of a Si substrate with aluminium foil during sputtering, then removing the foil from the substrate, thus creating a step in the coating. This step was measured using a profilometer. Energy Dispersive X-ray Spectroscopy (EDS) was used to determine the weight percentage of Si in the coatings. The phase structure of the coatings was identified using a vertical X-ray Diffractometer (XRD) with $CuK_\alpha$ radiation, operating at 40 kV and 40 mA. Data were collected over a $2\theta$ range from 20° to 40°,

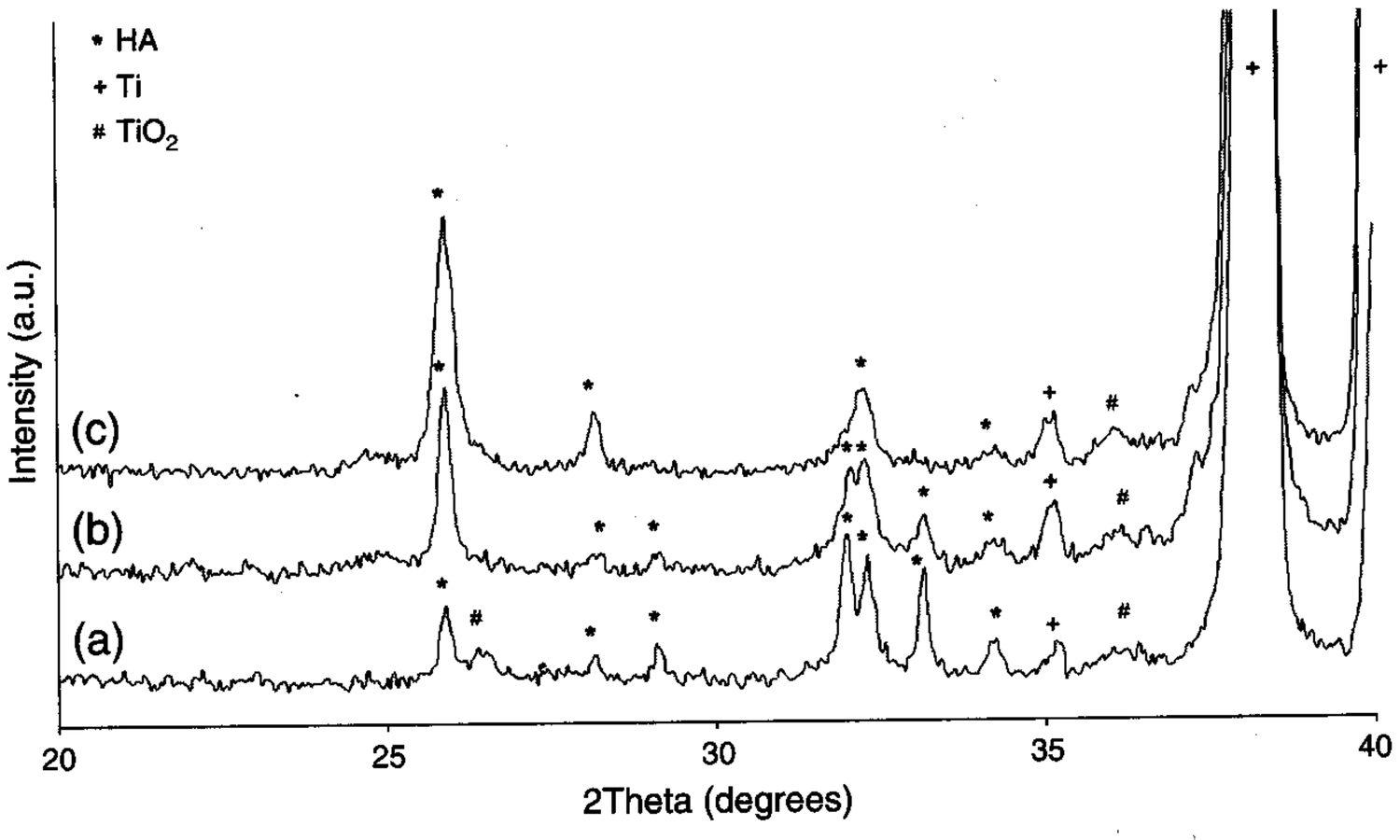


Fig. 1. XRD patterns of heat-treated Si–HA thin coatings. (a) 0.8 wt.% Si; (b) 2.2 wt.% Si; (c) 4.9 wt.% Si.

with a step size of 0.05° and a dwell time of 10 s. The molecular structure of the coatings was analysed using Fourier Transform Infrared Spectroscopy (FTIR). Spectra were collected over a range from 700 to 4000 $cm^{-1}$, utilising the grazing angle technique at a resolution of 4 $cm^{-1}$.

### 2.4. Cell culturing work

Human osteoblast-like cells (HOB, obtained from Promocell GmbH, Germany) were used. HOBs were cultured in McCoy's 5 A medium containing 10% foetal calf serum, 1% glutamine and Vitamin C (30 μg/ml). Si–HA coatings with different Si compositions were sterilised in ethanol for 48 h before treatment with ultra-violet radiation for 30 min. HOBs ($1 \times 10^4$ cells/test) were then seeded on the surfaces before incubating at 37 °C in a humidified atmosphere of 95% air and 5% carbon dioxide. HA coatings were used as a control in this work.

#### 2.4.1. Cell growth

At days 2 and 4, the metabolic activity of the cells on each sample was determined by the AlamarBlue™ assay (Serotec, Oxford, UK). The absorbance was measured on a plate reader at a wavelength of 570 nm. A total of 6 replications were performed for each sample.

#### 2.4.2. Cell organisation

At culture day 1, HOBs were fixed with 4% paraformaldehyde/phosphate buffer solution with 1% sucrose for 15 min, washed with phosphate buffer solution (PBS) and permeabilised at 4 °C for 5 min. Cells were then incubated with 1% bovine serum albumin (BSA)/PBS at 37 °C for 5 min to block the non-specific binding. FITC conjugated phalloidin (1:100 in 1% BSA/PBS, Sigma, Poole, UK) was concurrently added at this incubation duration. After washing with 0.5% Tween 20/PBS for 5 min, TOTO-3 (1:5000 in Tris/EDTA buffer at pH 8.0, Molecular Probes, Paisley, UK) was added at 24 °C for 5 min. The samples were given a final wash (5 min × 3) before mounting on the Vectorshield fluroscent mountants (Vector Laboratories, Peterborough, UK) and viewed under a Confocal Laser Scanning Microscope (CLSM).

#### 2.4.3. Cell morphology

At days 2 and 42, the cultured samples were rinsed with PBS before freeze-drying. They were then coated with a thin layer

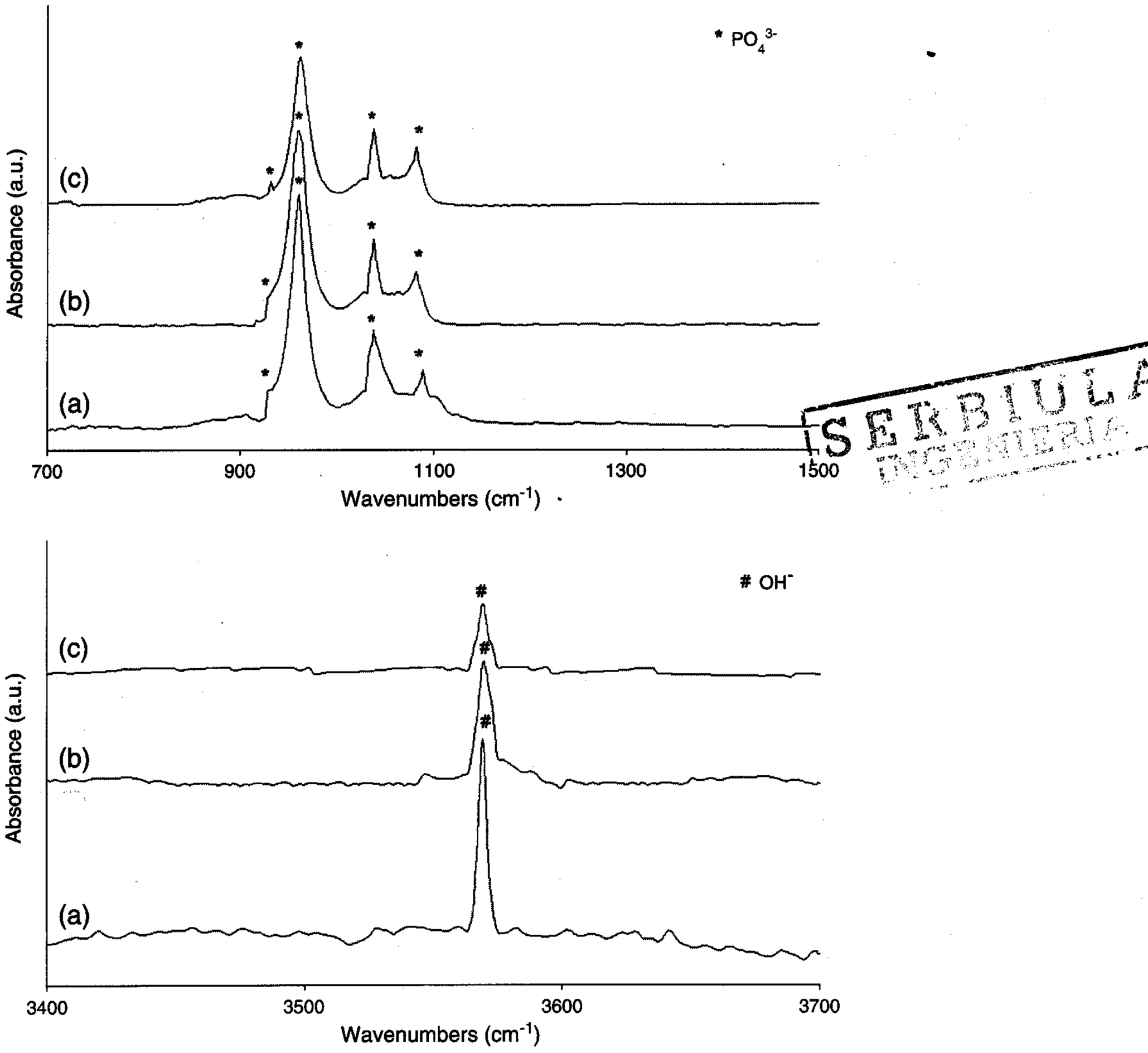


Fig. 2. FTIR spectra of heat-treated Si–HA thin coatings. (a) 0.8 wt.% Si; (b) 2.2 wt.% Si; (c) 4.9 wt.% Si.

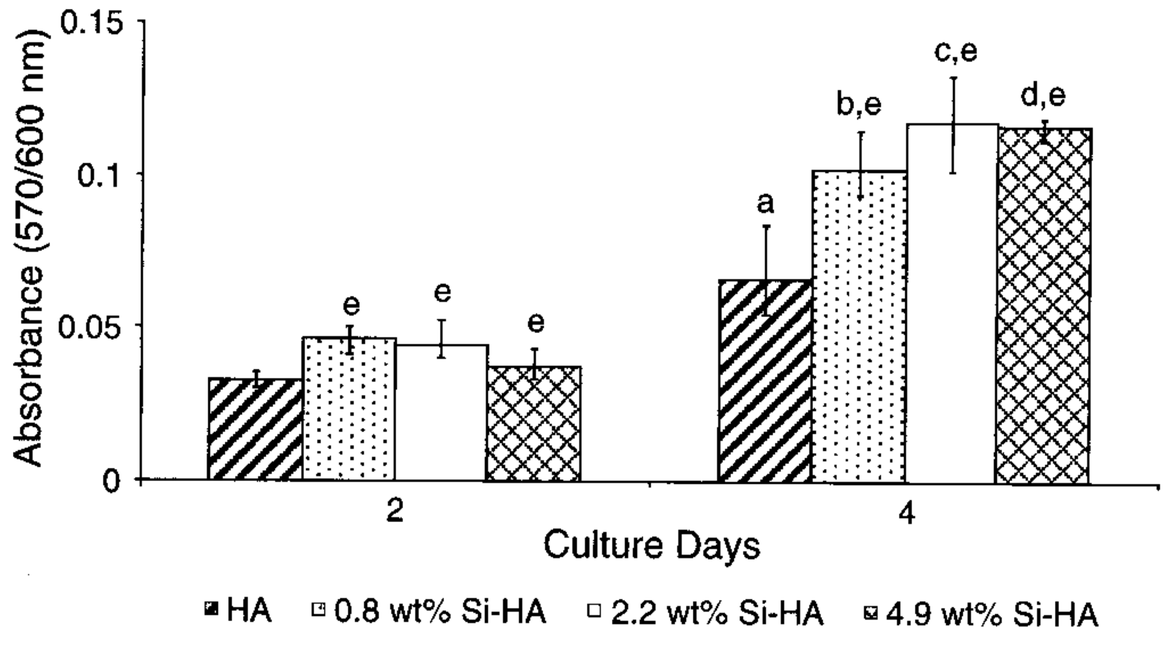


Fig. 3. Growth activity of HOBs at different time points. [a]$p<0.05$: Growth was significantly higher on HA between groups; [b]$p<0.05$: Growth was significantly higher on 0.8 wt.% Si–HA between groups; [c]$p<0.05$: Growth was significantly higher on 2.2 wt.% Si–HA between groups; [d]$p<0.05$: Growth was significantly higher on 4.9 wt.% Si–HA between groups; [e]$p<0.05$: Growth was significantly higher on Si–HA than HA within groups.

of carbon. The morphology of HOBs was examined using a Scanning Electron Microscope (SEM).

#### 2.4.4. Statistical analysis

A *t*-test was used to determine whether any significant differences existed between the mean values of the experimental groups. A difference between groups was considered to be significant at $p<0.05$.

## 3. Results and discussion

### 3.1. Physicochemical properties of heat-treated Si–HA

Hydroxyapatite (HA) thin coatings of different Si compositions were produced by magnetron co-sputtering at room temperature, followed by heat-treatment (Table 1). The Si content in the coating increased with dc power on the Si target, whilst the thickness of the coating remained approximately constant.

Single-phase, polycrystalline coatings were obtained after heat-treatment, exhibiting several X-ray diffraction peaks characteristic of HA (Fig. 1). This result is critical for thin coatings since it is well-known that amorphous CaP, tricalcium phosphate or tetracalcium phosphate have high solubilities, compared to HA [20,21]. If the coating is non phase-pure, there is a high probability that it will dissolve completely into the physiological environment, even before it is able to accelerate the promotion of direct attachment at the bone/implant interface. The Ti substrate was oxidised during heat-treatment, as evidenced by the presence of rutile titanium oxide ($TiO_2$) in the XRD patterns.

The FTIR spectra of the heat-treated Si–HA coatings are plotted in Fig. 2. Four typical absorption bands for HA were observed: one at 3571 $cm^{-1}$, associated with the presence of O–H; and the other three at 1089, 1038 and 962 $cm^{-1}$, assigned to the presence of P–O. An additional absorption band at 935 $cm^{-1}$ suggested the incorporation of Si into the apatite, which resulted

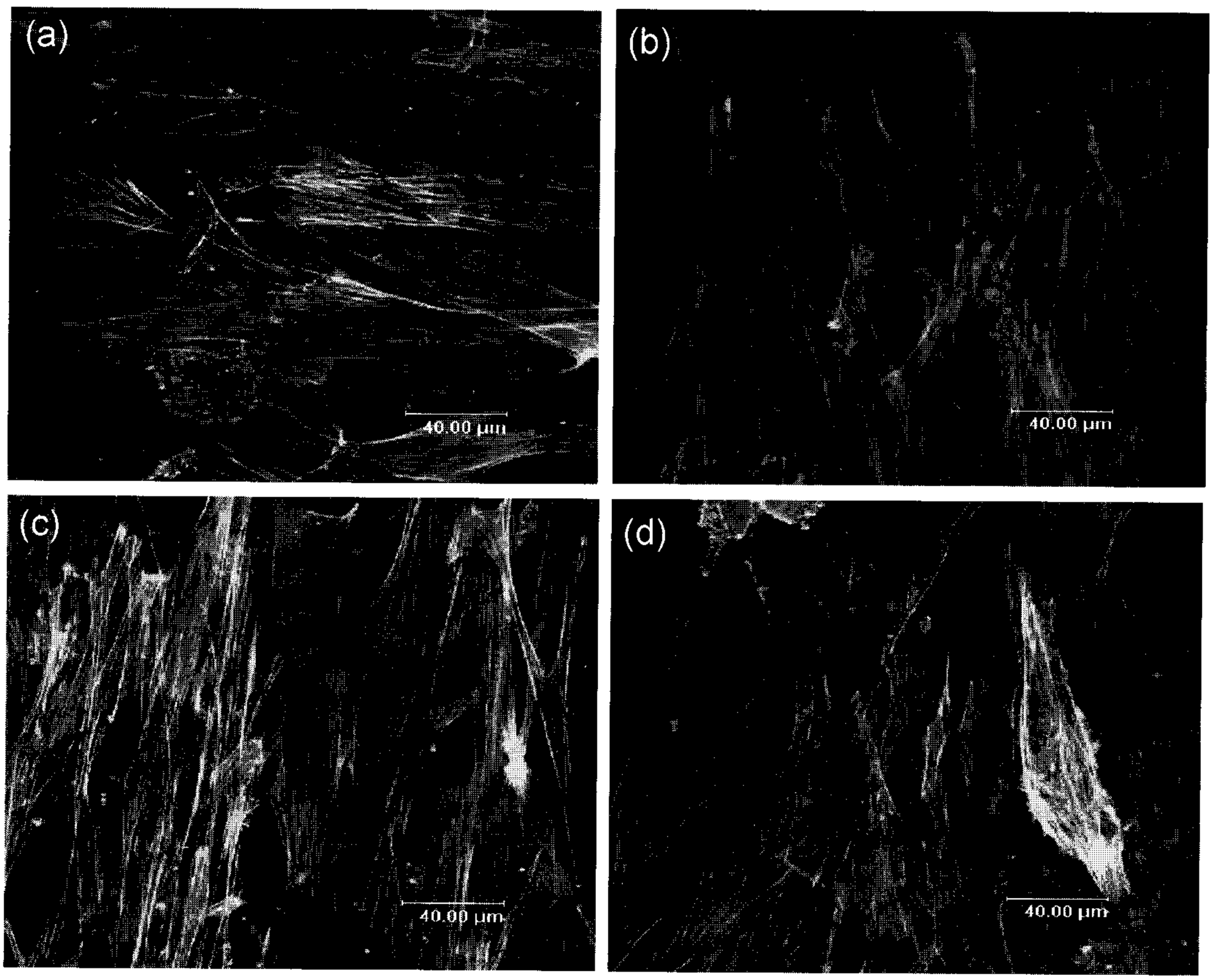


Fig. 4. Immunostained images of nuclear DNA (blue) and actin cytoskeleton (green) in HOB at day 1, as revealed with double labelling using TOTO-3 and FITC conjugated phalloidin. (a) 0.8 wt.% Si–HA; (b) 2.2 wt.% Si–HA; (c) 4.9 wt.% Si–HA; (d) HA. (For interpretation of the references to colour in this figure legend, the reader is referred to the web version of this article.)

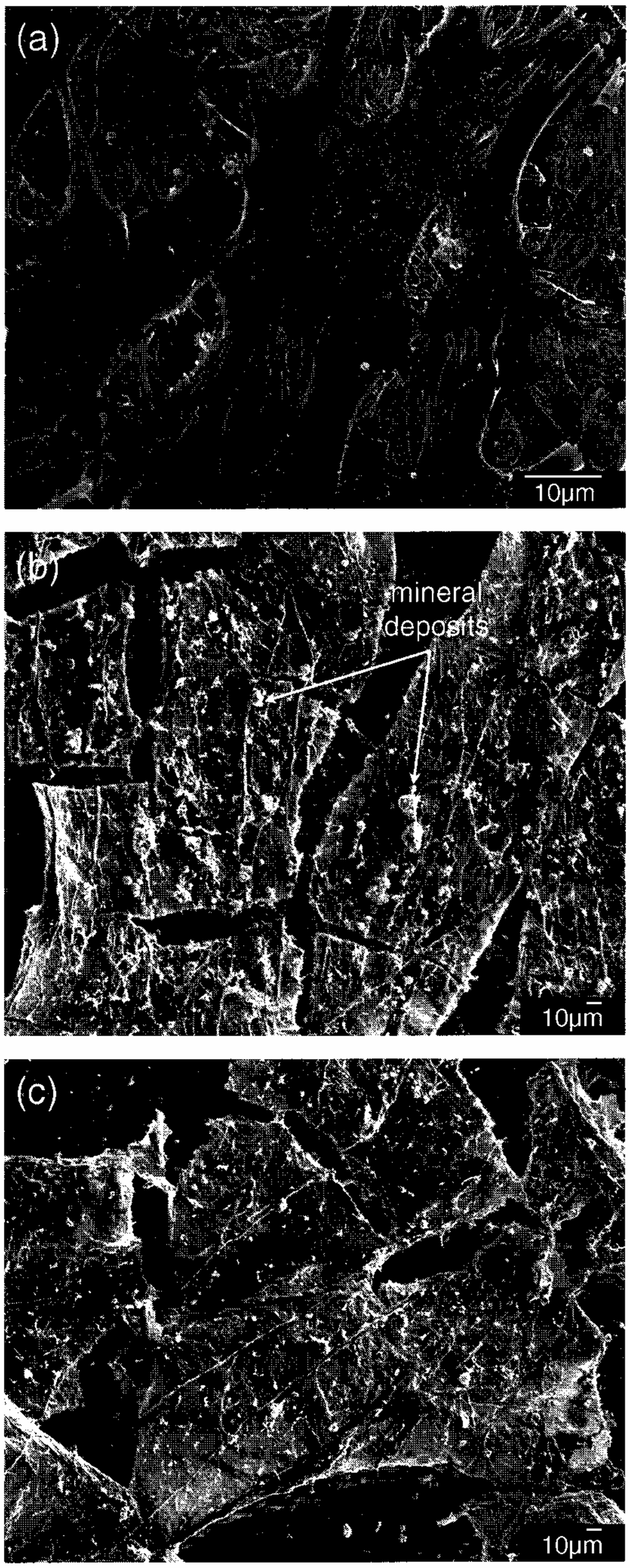


Fig. 5. SEM images of HOBs on various samples. (a) Monolayer of cells attaching on 0.8 wt.% Si–HA with the formation of extracellular matrices at culture day 2; Sign of mineralisation on (b) 4.9 wt.% Si–HA, and (c) HA at culture day 42.

in changes in the chemical bonding and symmetry of phosphate groups [22,23]. With increasing Si substitution, the band intensity corresponding to O–H and P–O (most noticeably at 962 $cm^{-1}$) decreased, suggesting that the silicate tetrahedra were substituting for the phosphate tetrahedra in the HA structure [22].

### *3.2. Biological properties of heat-treated Si–HA*

Osteoblast responses on various Si–HA coatings were compared with HA coatings (acting as controls in this study) in terms of cell growth, attachment and morphology. The AlamaBlue™ assay test indicated a significant increase in the growth of human osteoblast-like (HOB) cells with culturing time on all samples (Fig. 3). When comparison was made between Si–HA and HA, significant differences were noted at all time points, with Si–HA resulting in a higher HOB activity.

Immunostaining evaluation of HOBs attaching on coatings revealed that, by day 1, the actin cytoskeleton on Si–HA showed long and distinct microfilaments aligning along the long axis of the cells (Fig. 4a–c). In contrast, the organisation of the actin cytoskeleton on HA seemed diffuse, exhibiting fewer and shorter microfilaments throughout the cytoplasm (Fig. 4d).

The morphology of the HOB cells was analysed using scanning electron microscopy. By day 2, cells were spreading well and appeared to be flattened on both Si–HA and HA (Fig. 5a). In addition, extensive extracellular matrix (ECM) was formed throughout the surfaces. By day 42, CaP mineral deposits were formed primarily along the ECM, indicating signs of mineralisation. The level of mineral deposits on all Si–HA coatings appeared much higher than on HA (Fig. 5b,c).

All these results reflect the suitability of Si–HA coatings for cell attachment and growth. The presence of Si in Si–HA coatings has been shown to alter the surface properties of the material [24,25] which, in turn, could have a stimulatory effect on the biomineralisation process. In this study, it is hypothesised that a higher concentration of protein is adsorbed onto Si–HA than HA, owing to the formation of bound silicate network structure on Si–HA surface when the released silicon ions from the coatings combined with the oxygen ions, which has been shown having the capability of binding proteins together [26]. This effect resulted in differences in the interaction with integrins, and consecutively triggering specific signals. These signals can then regulate many cellular functions such as cell attachment, proliferation and differentiation, or even mobility and shape [27]. This phenomenon can be clearly seen from the present study where high cell growth, well-organised cytoskeletal architecture and enhanced biomineralisation were achieved on Si–HA. Studies by Keeting et al. [28] and Reffitt et al. [29] supported the current findings since they showed that soluble Si stimulated the proliferation and differentiation of cells and increased the production of collagen type I.

## 4. Conclusions

Magnetron co-sputtering has been successfully used for the production of silicon-substituted hydroxyapatite (Si–HA) thin coatings on titanium (Ti) substrates. Three different Si compositions were obtained: 0.8, 2.2 and 4.9 wt.%. X-ray and infrared analyses confirmed that, upon heat-treatment, these coatings formed a crystalline, single-phase apatite structure. The thin Si–HA coated layer on Ti substrates stimulated osteoblast attachment, proliferation and differentiation. Hence, these novel Si–HA thin coatings demonstrate a potential for use in orthopaedic and maxillo-facial applications.

## Acknowledgments

We would like to thank Girton College (Cambridge University), Cambridge Commonwealth Trust, Lee Foundation (Singapore),

and Sir Richard Stapley Educational Trust (UK) on behalf of the GlaxoSmithKline plc. for their financial support of EST. Conference support was provided by The Royal Academy of Engineering (UK), Armourers and Brasiers' Company (UK), Novelis UK, and The Royal Microscopical Society (UK), to enable EST to present this paper orally in the 3rd ICMAT and 9th IUMRS-ICAM held in Singapore.

## References

[1] L.L. Hench, J. Am. Ceram. Soc. 74 (1991) 1487.
[2] P. Ducheyne, Q. Qiu, Biomaterials 20 (1999) 2287.
[3] R.J. Furlong, J.F. Osborn, J. Bone Jt. Surg. 73B (1991) 741.
[4] J. Delecrin, G. Daculsi, N. Passuti, B. Duquet, Cells Mater. 4 (1994) 51.
[5] C.P. Klein, P. Patta, H.B. van der Lubbe, J.G. Wolke, K. de Groot, J. Biomed. Mater. Res. 25 (1991) 53.
[6] W.R. Lacefield, L.L. Hench, Biomaterials 7 (1986) 104.
[7] W.C.A. Vrouwenvelder, C.G. Groot, K. de Groot, Biomaterials 13 (1992) 382.
[8] A. Oliva, A. Salerno, B. Locardi, V. Riccio, F. Dells Ragione, P. Iardino, V. Zappia, Biomaterials 19 (1998) 1019.
[9] M. Nagase, Y. Abe, M. Chigira, E. Udagawa, Biomaterials 13 (1992) 172.
[10] H.B. Wen, J.R. de Wijn, C.A. van Blitterswijk, K. de Groot, J. Biomed. Mater. Res. 46 (1999) 245.
[11] M. Lind, S. Overgaard, T. Nguyen, B. Ongpipattanakul, C. Bunger, K. Soballe, Acta Orthop. Scand. 67 (1996) 611.
[12] J.W.M. Vehof, J.D.D.S. Mahmood, H. Takita, M.A. van't Hof, Y. Kuboki, P.H.M. Spauwen, J.A. Jansen, Plast. Reconstr. Surg. 108 (2001) 434.
[13] M. Yazdi, S. Bernick, W.J. Paule, Clin. Orthop. 262 (1991) 281.
[14] E.S. Thian, J. Huang, S.M. Best, Z.H. Barber, W. Bonfield, J. Mater. Sci. Mater. Med. 16 (2005) 411.
[15] E.S. Thian, J. Huang, S.M. Best, Z.H. Barber, W. Bonfield, Biomaterials 26 (2005) 2947.
[16] E.M. Carlisle, Science 178 (1972) 619.
[17] E.M. Carlisle, Fed. Proc. 32 (1973) 930.
[18] E.M. Carlisle, J. Nutr. 110 (1980) 1046.
[19] K.F. Orishimo, A.M. Claus, C.J. Sychterz, C.A. Engh, J. Bone Jt. Surg. Am. 85A (2003) 1095.
[20] M. Jarcho, Clin. Orthop. 157 (1981) 259.
[21] F.C. Driessens, Ann. N. Y. Acad. Sci. 523 (1988) 131.
[22] I.R. Gibson, S.M. Best, W. Bonfield, J. Biomed. Mater. Res. 44 (1999) 422.
[23] Th. Leventouri, C.E. Bunaciu, V. Perdikatsis, Biomaterials 24 (2003) 4205.
[24] A.E. Porter, N. Patel, J.N. Skepper, S.M. Best, W. Bonfield, Biomaterials 24 (2003) 4609.
[25] C.M. Botelho, M.A. Lopes, I.R. Gibson, S.M. Best, J.D. Santos, J. Mater. Sci. Mater. Med. 13 (2002) 1123.
[26] W. Schwarz, Fed. Proc. 33 (1974) 1748.
[27] B.G. Keselowsky, D.M. Collard, A.J. Garcia, J. Biomed. Mater. Res. 66A (2003) 247.
[28] P.E. Keeting, M.J. Oursler, K.E. Wiegand, S.K. Bonde, T.C. Spelsberg, B.L. Riggs, J. Bone Miner. Res. 7 (1992) 1281.
[29] D.M. Reffitt, N. Ogston, R. Jugdaoshsingh, H.F.J. Cheung, B.A.J. Evans, R.P.H. Thompson, J.J. Powell, G.N. Hampson, Bone 32 (2003) 127.